ARTICLE

ACT001 inhibits pituitary tumor growth by inducing autophagic cell death via MEK4/MAPK pathway

Lin Cai[1], Ze-rui Wu[1], Lei Cao[2], Jia-dong Xu[3], Jiang-long Lu[1], Cheng-de Wang[1], Jing-hao Jin[1], Zhe-bao Wu[1,4] and Zhi-peng Su[1]

ACT001, derived from traditional herbal medicine, is a novel compound with effective anticancer activity in clinical trials. However, little is known regarding its role in pituitary adenomas. Here, we demonstrated that ACT001 suppressed cell proliferation and induced cell death of pituitary tumor cells in vitro and in vivo. ACT001 was also effective in suppressing the growth of different subtypes of human pituitary adenomas. The cytotoxic mechanism ACT001 employed was mainly related to autophagic cell death (ACD), indicated by autophagosome formation and LC3-II accumulation. In addition, ACT001-mediated inhibitory effect decreased when either ATG7 was downregulated or cells were cotreated with autophagy inhibitor 3-methyladenine (3-MA). RNA-seq analysis showed that mitogen-activated protein kinase (MAPK) pathway was a putative target of ACT001. Specifically, ACT001 treatment promoted the phosphorylation of JNK and P38 by binding to mitogen-activated protein kinase kinase 4 (MEK4). Our study indicated that ACT001-induced ACD of pituitary tumor cells via activating JNK and P38 phosphorylation by binding with MEK4, and it might be a novel and effective anticancer drug for pituitary adenomas.

Keywords: ACT001; pituitary adenoma; autophagic cell death; MEK4; P38; JNK

INTRODUCTION

Pituitary adenoma is one of the most common intracranial neoplasms, and ~40% to 66% of all pituitary adenomas are prolactinomas [1, 2]. Although ~75% to 90% of prolactinoma cases can benefit from dopamine agonists (DAs) treatment [1–4], some patients still have little or no response to treatment of DAs. Therefore, it is an objective requirement to develop new therapeutic drugs for pituitary adenomas.

ACT001 (also known as dimethylamino-micheliolide, i.e., DMAMCL) is certified as an orphan drug by the Food and Drug Administration in the United States [5, 6]. It is derived from micheliolide (MCL), a guaianolide sesquiterpene lactone isolated from *Michelia compressa* and *Michelia champaca*, and it has notable anticancer properties and is effective in the treatment of glioblastoma [7–9], acute myelogenous leukemia [5, 10], breast cancer [11] and melanocytoma [12]. DMAMCL is the dimethyla-mino Michael adduct of MCL and ACT001 is a fumarate salt form of DMAMCL [13]. After administration, ACT001 can be hydrolyzed to produce DMAMCL by esterase, a type of catalyzing enzyme exists abundantly in intestines, liver and plasma. Then DMAMCL can slowly but consistently release MCL in plasma and organs in vivo (Fig. 1a) [13, 14]. ACT001, acting as a water-soluble prodrug of MCL typically used in vivo, displays relatively higher plasma stability, more sustained release and superior efficacy, which increases its oral bioavailability and enhances its therapeutic efficiency [15]. However, the role and molecular mechanism of ACT001 in the treatment of pituitary adenomas remains unknown.

In the present study, we aimed to investigate the anticancer effects and the underlying mechanisms of ACT001 in pituitary tumors. We found that ACT001 induced autophagy-dependent cell death of pituitary tumor cells in vitro and in vivo via promoting the phosphorylation of JNK and P38 by binding to MEK4. Moreover, ACT001 could exert its inhibitory effect in different subtypes of primary human pituitary adenomas. These novel findings provide new insight into therapies and pharmacological strategies to overcome the drug resistance of pituitary adenomas.

MATERIALS AND METHODS

Cell culture and reagents

The rat pituitary tumor cell lines GH3 (ATCC CCL-82.1™; Manassas, VA) and MMQ (ATCC CCL-10609™; Manassas, VA) were purchased from the American Type Culture Collection, cultured in Ham's F-12K (Kaighn's) Medium (Gibco, USA, #21127030) supplemented with 2.5% fetal bovine serum (FBS, Gibco, USA, #10100-147), 15% horse serum (HS, Gibco, USA, #16050-122) and 100 U/mL penicillin/streptomycin (Gibco, USA, #15070-063), and incubated in a humidified incubator at 37 °C in 5% (v/v) CO_2.

GH3 cells, a double dicentric marker chromosomes cell line derived from a 7-month-old female Wistar-Furth rat in 1965 [16], which have the advantages of epithelial-like morphological characteristics and possess the ability of tumor formation in nude mice. The growth properties of GH3 cells are loosely adherent with

[1]Department of Neurosurgery, The First Affiliated Hospital of Wenzhou Medical University, Wenzhou 325000, China; [2]Department of Neurosurgery, Beijing Tiantan Hospital, Capital Medical University, Beijing 100050, China; [3]Department of Cardio-Thoracic Surgery, Zhoushan Hospital, Zhoushan 316021, China and [4]Department of Neurosurgery, Center of Pituitary Tumor, Ruijin Hospital, Shanghai Jiao Tong University School of Medicine, Shanghai 200025, China
Correspondence: Zhe-bao Wu (zhebaowu@aliyun.com) or Zhi-peng Su (drsuzhipeng@163.com)
These authors contributed equally: Lin Cai, Ze-rui Wu, Lei Cao

floating clusters. The cells generate growth hormone at a great rate and also produce a small amount of prolactin as well [17, 18].

MMQ cells, a prolactin-secreting clonal pituitary cell line isolated from the 7315a rat pituitary tumor tissue, express functional dopamine 2 receptor (DRD2). Light microscopic examination reveals rounded or irregular tumor cells possessing large spherical nuclei and prominent nucleoli. The cells can exert its tumorigenic ability in nude mice with semisolid medium and the MMQ tumors only increase the levels of serum prolactin without affecting the levels of other pituitary hormones or corticosterone in vivo. MMQ cells grow mainly in the state of suspension [19].

ACT001 was generously provided by Accendatech Co., Ltd. (Tianjin, China) and dissolved in sterile water. The reagents used in this study were shown in Supplementary Table S1.

Pituitary tumor tissue collection

This study was approved by the Clinical Research Ethics Committee of First Affiliated Hospital of Wenzhou Medical University (permission: 2016-082), and written informed consent was obtained from all patients. Postsurgical pituitary adenoma tissue specimens were collected from June 2019 to August 2020. Tumors were classified by histopathological and immunohisto-chemical analysis according to the World Health Organization classification of tumors of the pituitary gland (2017 edition) [20]. Fourteen pituitary tumor tissues were obtained for primary tumor cell culture. The clinical characteristics of the patients were shown in Supplementary Table S2.

For the isolation of primary human pituitary tumor cells, all steps were carried out under sterile conditions in a laminar flow cell culture hood to reduce the risk of contamination of the primary culture. Firstly, the tumor specimens were washed with phosphate buffered saline (PBS, Gibco, USA, #70011069) and dissected into small fragments. Then, the fragments were enzymatically digested by using human Tumor Dissociation kit (Miltenyi Biotec, Germany, #130-095-929) in combination with the gentleMACS™ Dissociator (Miltenyi Biotec, Germany, #DXT-130-096-730). Fibroblasts containing in the cell suspension were removed by using human Anti-Fibroblast MicroBeads (Miltenyi Biotec, Germany, #130-050-601) and erythrocytes were removed by using Red Blood Cell Lysis Solution (10×) (Miltenyi Biotec, Germany, #130-094-183). Finally, a total of 1×10^6 cells were seeded in T25 cell culture flasks with a medium composed of DMEM medium (Gibco, USA, #8121300), 10% FBS and 100 U/mL penicillin/streptomycin at 5% (v/v) CO_2 humidified atmosphere with 37 °C for further research.

Cell viability assays and cell death analysis by flow cytometry

Cell viability was measured by Cell Counting Kit-8 (CCK-8) assay (Dojindo, Japan, #CK04). Cells (5000–10,000 per well) were seeded into 96-well plates overnight and then treated with ACT001. At indicated time after treatment, 10 μL CCK-8 solution was added to 90 μL of culture medium. The cells were subsequently incubated for 3 h and the absorbance was measured at 450 nm by using a microplate luminometer (TECAN, Switzerland). Besides that, the half maximal inhibitory concentration (IC_{50}) value of ACT001 was assessed according to the relative survival curve.

To determine the effect of ACT001 on apoptosis, a FITC-Annexin V apoptosis detection kit I (BD Biosciences, USA, #559763) was used according to manufacturer's instructions. First, the cells were exposed to ACT001 for 0–48 h. Next, a total of ≥10,000 cells were resuspended in binding buffer and incubated with 5 μL of Annexin V-FITC and 5 μL of PI for 15 min in dark conditions. The proportions of cells in early apoptosis and late apoptosis were reported as the percentage of Annexin V^+/PI^-- and Annexin V^+/PI^+-labeled cells, respectively. The stained cells were analyzed directly by flow cytometry using a FACSCalibur with the Cell Quest program (BD Biosciences, USA) for data analysis.

Xenograft animals and rat prolactinoma model

Five-week-old female BALB/c (*nu/nu*) athymic nude mice were purchased from Shanghai Experimental Animal Center (Shanghai, China). GH3 cells (5×10^6) were resuspended in PBS with Matrigel (1:1; BD Biosciences, USA, #356234) and then subcutaneously injected into the left back of each nude mouse. All mice had free access to food and water. When the transplanted tumors reached an average size of 50 mm³, the mice were randomly assigned to two groups. Before drug administration, mice were fasted for 12 h and given free access to water. Vehicle or ACT001 was administered (100 mg/kg) daily by oral gavage. Tumor volumes were measured with calipers at two perpendicular diameters and calculated individually using the formula (length × width²)/2. Twenty-nine days later, all mice were sacrificed, and tumors were harvested, photographed and processed for Western blotting.

For rat prolactinoma model, tumors were induced by sub-cutaneously implanting 1-cm silastic capsules containing 10 mg of 17β-estradiol into Fischer 344 rats (female, 4 weeks old) [21]. Prolactinomas were induced by 17β-estradiol release for 6 weeks, as reported by Wu et al. [22]. Five weeks later, all rat pituitary tumors were validated via magnetic resonance imaging (MRI) before administration of ACT001 (200 mg/kg) daily by oral gavage. Two weeks later, after undergoing MRI examinations to measure tumor size, all rats were sacrificed, and tumor tissues were collected for further assessments.

All procedures were approved by the Administration Commit-tee of Experimental Animals, Laboratory Animal Center, Wenzhou Medical University (Permit Number: wydw2019-0302).

Immunoblotting

Cells and tumor samples were extracted with cell lysis buffer (Beyotime, China, #P0013J), and the protein concentrations in the lysates were quantified using an Enhanced BCA Protein Assay Kit (Beyotime, China, #P0010). Protein samples (30–50 μg) were separated by SDS-PAGE and then transferred to PVDF membranes (Millipore, USA, #IPVH00010). The membranes were immuno-blotted with primary antibodies followed by HRP-conjugated secondary antibodies. Immunoreactive proteins were visualized using an ECL Western blot detection kit (Advansta, USA, #K-12045-D50), and images were developed using a Bio-Rad system (Bio-Rad, USA). The indicated antibodies were listed in Supplementary Table S1 and statistical results of Western blot analyses were shown in Supplementary Figs. S2, S3.

Transmission electron microscopy (TEM)

Samples were processed in the Electron Microscopy Department at Wenzhou Medical University. Cell pellets were fixed with 2.5% glutaraldehyde overnight in 0.1 M phosphate buffer and postfixed with 1% osmium tetroxide (pH 7.4) for 2 h at room temperature. The pellets were then dehydrated in a graded ethanol series and infiltrated with Spurr's resin (Polysciences, USA, #01916-1) to embed the tissues. Samples were then polymerized for 48 h at 60 °C, cut into 60-nm-thick sections on an LKB-I microtome (LKB, Sweden), positioned on 200-mesh grids (Polysciences, USA, #22896-1), and stained with uranyl acetate and lead citrate. TEM was performed on a PHILIPS CM120 transmission electron microscope at an accelerating voltage of 120 kV. Images were acquired with a Gatan-type UltraScan 4000SP CCD camera connected to the microscope.

Immunofluorescence staining

Cultured cells seeded on coverslips were fixed with 4% paraformaldehyde for 20 min and incubated in blocking buffer for 1 h. Next, coverslips were incubated overnight with primary antibodies at 4 °C followed by PE-conjugated secondary anti-bodies (Santa Cruz, USA, #sc-3745), after which they were stained with DAPI solution (Sigma-Aldrich, USA, #D9542). Staining was

2388

visualized on an LSM710 laser scanning confocal microscope with a 363-oil immersion lens (Carl Zeiss, Oberkochen, Germany), and images were obtained.

Gene silencing
The rat prolactinoma cell lines MMQ and GH3 were transfected with small interfering RNAs (siRNAs) using Lipofectamine RNAiMAX (Invitrogen, USA, #13778150). siRNAs against rat ATG7 were from GenePharma (Shanghai, China). The sequences of the siRNAs were as follows:

siATG7: 5′-CAGCCUGGCAUUUGAUAAATT-3′
5′-UUUAUCAAAUGCCAGGCUGTT-3′
siControl: 5′-UUCUCCGAACGUGUCACGUTT-3′
5′-ACGUGACACGUUCGGAGAATT-3′

RNA-sequence array
In total, 3 µg of RNA per sample was used as input material for the preparations. Sequencing libraries were generated using the NEB Next® Ultra™ RNA Library Prep Kit for Illumina® (NEB, USA, #E7530L) following the manufacturer's recommendations, and index codes were added to attribute sequences to each sample. Clustering of the index-coded samples was performed on a cBot Cluster Generation System using a TruSeq PE Cluster Kit v3-cBot-HS (Illumina, USA, #PE-401-3001). After cluster generation, the library preparations were sequenced on an Illumina platform, and 125 bp/150 bp paired-end reads were generated.

Histology and IHC
The tumor tissues were harvested, fixed in 4% paraformaldehyde for 24 h, embedded in paraffin, and serially sectioned (4 µm). For hematoxylin and eosin (H&E) staining, sections were stained with H&E (Beyotime, China, #P0010). For IHC, the tissue sections were dehydrated and subjected to peroxidase blocking before primary antibodies were added and incubated at room temperature for 30 min on a Dako AutoStainer using the Dako Cytomation EnVision+ System-HRP (DAB) detection kit (Carpinteria, USA, #K406511-2). The slides were counterstained with hematoxylin before they were observed under a microscope (Leica, Germany), and images were acquired.

Liquid chromatography–mass spectrometry (LC–MS) and pull-down of ACT001-biotin bound proteins
ACT001-biotin-bound proteins were isolated as described previously [14, 23]. We constructed ACT001-biotin probe as positive group and ACT001-S-biotin probe as negative group. GH3 and MMQ cells were harvested and lysed with RIPA buffer (Beyotime, P0013C) and centrifuged at 4 °C. The supernatant (1.5 mg/mL) was collected and equally divided into four samples. One supernatant sample was incubated with 100 µM ACT001-biotin in RIPA buffer, and immunoprecipitates were separated by SDS-PAGE. The band was excised, subjected to in-gel trypsin digestion and then analyzed by LC–MS analysis using Q Exactive™ (Thermo Scientific, USA, #IQLAAEGAAPFALGMAZR). The scan rates were up to 12 Hz, and the scan range was from 250–1500 m/z. LC–MS spectra were searched against the concatenated target and decoyed Swiss-Prot protein database using Proteome Discoverer Software (Thermo Scientific). Peptides passing a false discovery rate threshold of 1% were accepted.

The other three samples were used in the protein pull-down assay. One supernatant sample was used as input group. The other two samples were either incubated with 100 µM ACT001-biotin or ACT001-S-biotin in lysis buffer overnight at 4 °C. Then, the samples were incubated with pre-washed Streptavidin Agarose Beads (20349, Thermo Fisher, USA) for 1 h at room temperature. Then these beads-bound proteins were eluted and separated by SDS-PAGE, and visualized by silver staining and Western blot.

Statistical analysis
All statistical analyses were carried out using the SPSS 16.0 statistical software package (SPSS Inc., Chicago, IL, USA). Continuous variables were expressed as the means ± SEM. In each experiment, all conditions were evaluated at least in triplicate. Statistical significance between two measurements was determined by the two-tailed unpaired Student's t test, and among groups of three or more, it was determined by one-way analysis of variance (ANOVA). P values < 0.05 were considered statistically significant.

RESULTS

ACT001 inhibited the growth of pituitary tumor cells
Plenty of studies have shown that ACT001 had notable anticancer properties [5, 6, 11, 14, 24]. In order to clarify the role of ACT001 in the treatment of pituitary adenomas, we treated the rat pituitary tumor cell lines (GH3 and MMQ cells) and primary human pituitary adenomas with ACT001. Subsequently, CCK-8 assays showed that the viability of GH3 and MMQ cells markedly decreased in both a dose- (Fig. 1b, $P < 0.001$) and time-dependent (Fig. 1c, $P < 0.01$, $P < 0.001$) manner in response to ACT001 treatment. The IC_{50} value of ACT001 for 24 h was 9.56 µM in GH3 cells and 22.65 µM in MMQ cells. Furthermore, the results of Annexin V/PI apoptosis assay demonstrated that ACT001 increased the rate of apoptosis in GH3 and MMQ cells as a time-dependent manner (Supplementary Fig. S1a, b). Next, we investigated the cytotoxic effect of ACT001 on primary human pituitary adenomas collected from 14 individuals (Supplementary Table S2 and Supplementary Fig. S2a). As shown in Fig. 1d, after being treated for 48 h, ACT001 (20 µM) resulted in a decrease in viability in 11 out of the 14 primary human pituitary adenomas, including 1 prolactin-secreting pituitary adenoma, 1 growth hormone-secreting pituitary adenoma and 9 clinically nonfunctioning pituitary adenomas. Intriguingly, ACT001 successfully inhibited the proliferation of DA-resistant prolactinoma primary cells (Case No. 1 in Supplementary Table S2).

These results indicated that ACT001 possessed a potent inhibitory effect on the growth of pituitary tumor cell lines. Moreover, ACT001 had obvious therapeutic effect on different subtypes of human primary pituitary adenoma cells, including DA-resistant tumors.

ACT001 suppressed pituitary tumor tumorigenesis in vivo
The GH3 xenograft and rat pituitary tumor in situ models were conducted to evaluate the effect of ACT001 in vivo. The GH3 xenograft experiments showed that the average tumor volume and weight of ACT001 treatment group were lower than that of the control group after inoculation for 29 days (154.83 ± 68.90 mm³ vs. 517.44 ± 217.60 mm³, $n = 6$, $P < 0.001$; Fig. 1e, f). Tumor weights were 0.09 ± 0.03 g and 0.33 ± 0.17 g in ACT001 treatment group and control group, respectively ($P = 0.012$, Fig. 1g). Next, we generated rat pituitary tumor in situ models by administering estrogen to Fischer 344 rats [21, 22]. MRI results showed that the volumes of tumors treated with ACT001 were smaller than the volumes of those in control rats (25.03 ± 4.89 mm³ vs. 30.60 ± 5.90 mm³; $n = 9$; $P = 0.045$; Fig. 1h, i). The tumor weights were 10.89 ± 0.78 mg and 12.22 ± 0.67 mg in ACT001 and control groups, respectively ($n = 9$, $P = 0.001$, Fig. 1j). Taken together, these results suggested that ACT001 effectively inhibited pituitary tumor progression in vivo.

ACT001 treatment results in autophagy induction
Accumulating evidence has shown that ACT001-induced autophagy played a crucial role in the regulation of tumor growth [11, 25, 26]. To investigate the mechanisms underlying the treatment of ACT001 in pituitary tumor cells, we evaluated the status of autophagy in pituitary tumor cells. As shown in Fig. 2a, b,
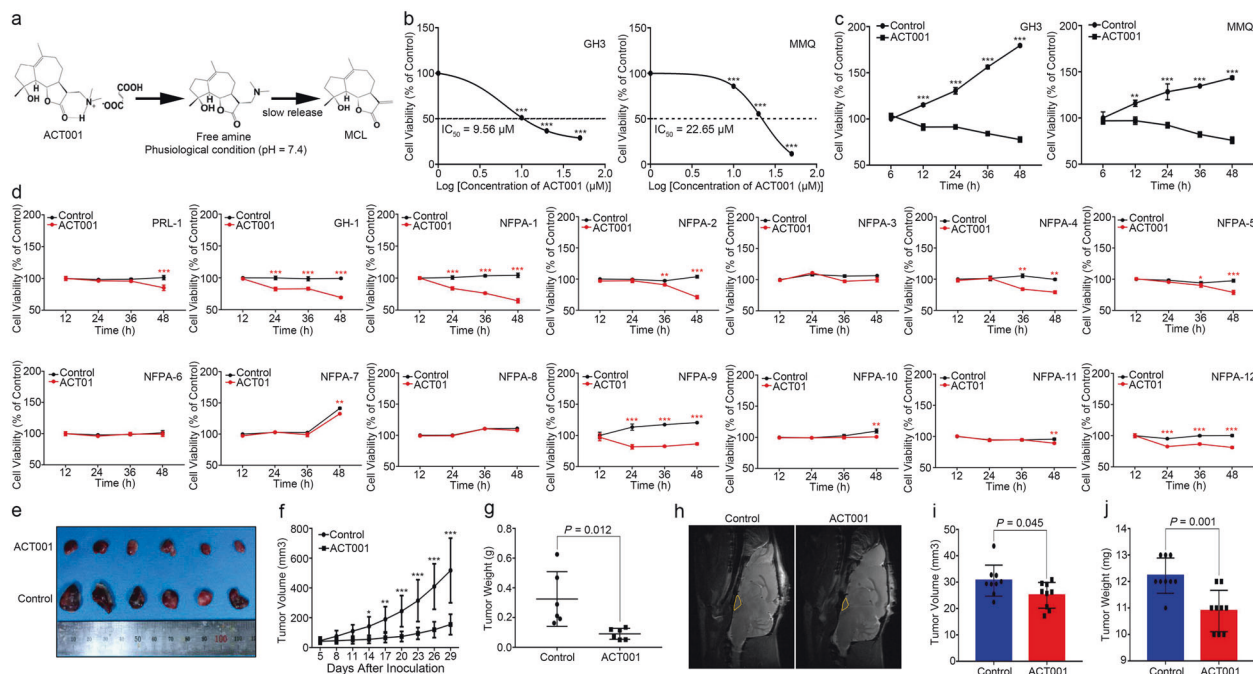
Fig. 1 ACT001 inhibited the growth of pituitary tumor cells in vitro and in vivo. a The mechanism of sustainable release of MCL by ACT001 under neutral conditions. The chemical structure of ACT001 and MCL were shown as indicated. **b**, **c** The suppressive effect of ACT001 on proliferation was determined by CCK-8 assay. As ACT001 concentration increased, the viability of GH3 cells (**b**, left) and MMQ cells (**b**, right) decreased. The IC_{50} value of ACT001 was assessed according to the relative survival curve. GH3 cells (**c**, left, 10 μM) and MMQ cells (**c**, right, 20 μM) were treated with ACT001 for 6–48 h and subjected to cell proliferation assay. The inhibitory effect of ACT001 on GH3 and MMQ cells increased markedly over time. **d** Primary cultures of 14 human pituitary adenomas were treated with 20 μM ACT001. The cell viability was measured at the indicated time points with the CCK-8 assay. ACT001 decreased the cell viability in 11 of 14 primary human pituitary tumor cultures. **e**–**g** ACT001 treatment (100 mg/kg, daily by oral gavage) inhibited the growth of subcutaneously transplanted GH3 cell tumors in nude mice. Representative images of xenograft tumors from nude mice were shown in (**e**), and tumor growth curves and tumor weights were shown in (**f**) and (**g**), respectively (n = 6). **h**–**j** ACT001 exerted therapeutic effects on in situ rat pituitary tumors. When pituitary tumors were induced by 17β-estradiol for 5 weeks, tumor-bearing rats were treated with ACT001 (200 mg/kg, daily by oral gavage). Two weeks later, tumor size was measured by MRI (orange circles) (**h**), after which the tumors (n = 9) were dissected, and tumor volume (**i**) and tumor weight (**j**) were calculated, the data were presented as the means ± SEM. ***$P < 0.001$; **$P < 0.01$; *$P < 0.05$ vs. control group.

ACT001 increased the expression levels of ATG7, P62 and LC3-II in both GH3 and MMQ cells in a time- (Fig. 2a and Supplementary Fig. S3a) and dose- (Fig. 2b and Supplementary Fig. S3b) dependent manner. We also assessed the expression of these proteins in 14 primary human pituitary adenoma cell samples. As shown in Supplementary Fig. S2b, c, Western blotting demonstrated that after ACT001 treatment, protein expression levels of ATG7, P62, and LC3-II increased in the majority of ACT001-sensitive human pituitary adenomas. This notion was also supported by the autolysosome observed and the formation of LC3 puncta (Fig. 2c, d).

To further validate whether ACT001-induced autophagy was a physiologically and pathologically important process in vivo, we measured the levels of autophagy-related proteins, ATG7, P62 and LC3II, in xenograft tumors and in situ tumors. As shown in Fig. 2e, f, tumors from ACT001-treated mice showed remarkable increase in the protein expression of ATG7, P62 and LC3-II compared with the control group. The statistical results of Western blot analyses were shown in Supplementary Fig. S3c, d. All the results suggested that ACT001 could promote autophagic level of pituitary tumor cells in vitro and in vivo.

Autophagic cell death participated in ACT001-induced cell death
To further confirm whether increased autophagy was involved in ACT001-induced cell death, we transfected siRNA to knockdown ATG7, which was essential for autophagy activation, in GH3 and MMQ cells [27]. As shown in Fig. 3a, b, the knockdown of ATG7 expression decreased the protein level of P62 and alleviated the conversion of LC3-I to LC3-II. In addition, the knockdown of ATG7

partially reversed ACT001-induced cell death in GH3 and MMQ cells. Compared with ACT001 treatment group, ACT001+siATG7 treatment group showed increased cell viability by 37.05% in GH3 cells ($P < 0.001$, Fig. 3a and Supplementary Fig. S3e) and by 22.40% in MMQ cells ($P < 0.001$, Fig. 3b and Supplementary Fig. S3f) at 24 h after treatment.

To determine the role of the autophagic induction in the regulation of ACT001-induced inhibition of GH3 and MMQ cells growth, 3-methyladenine (3-MA), a widely used inhibitor of autophagy via its inhibitory effect on class III PI3K, was employed [27]. Compared with ACT001 treatment alone, combined treatment with ACT001 and 3-MA markedly decreased the levels of P62 and LC3-II, and increased the viability of GH3 and MMQ cells by 39.58% ($P < 0.001$, Fig. 3c and Supplementary Fig. S3g) and 27.42% ($P < 0.001$, Fig. 3d and Supplementary Fig. S3h), respectively. These results indicated that ACT001-induced ACD participated in its inhibitory effect on the growth of pituitary tumor cells.

**ACT001 promoted the phosphorylation of JNK and P38 in pituitary tumor cells**
To further determine the underlying molecular mechanism by which ACT001 inhibited pituitary tumor growth, we carried out an RNA-sequence array of GH3 cells in the ACT001-treated group and control group. The clustering analysis results showed that 483 genes were downregulated (fold change > 1.2) and 125 genes were upregulated (fold change > 1.2) in the ACT001-treat group compared with the control group (Fig. 4a, listed in Supplementary Table S3). Moreover, KEGG pathway analysis clearly indicated that MAPK signaling pathway was mainly involved in the activity of
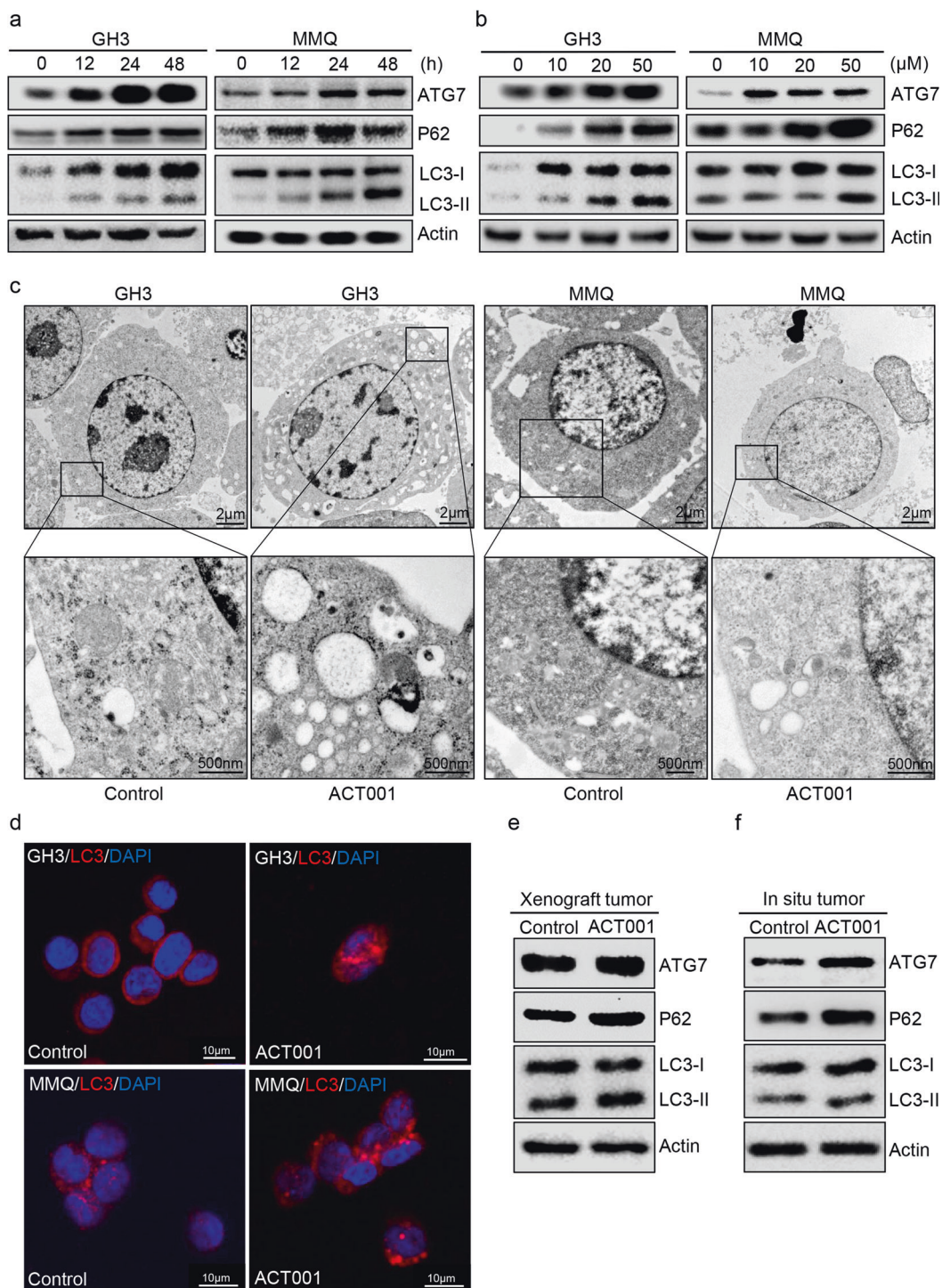
Fig. 2 ACT001 induced autophagy in rat pituitary tumor cells. a, **b** ACT001 promoted autophagy in a time- (**a**) and dose- (**b**) dependent manner. The protein levels of ATG7, P62, LC3-I, and LC3-II in GH3 and MMQ cells were determined by Western blot analysis, and actin was used as a control for protein loading. **c** Electron micrographs of GH3 and MMQ cells with or without ACT001 treatment for 24 h. Enlarged images of ACT001-treated cells (bottom row) indicated autolysosomes. **d** ACT001 treatment for 24 h induced punctate distribution of membrane-associated lipidated LC3-II in GH3-LC3 (top panels) and MMQ-LC3 (bottom panels) cells, as observed under a confocal microscope. **e**, **f** Immunoblot analyses showed ATG7, P62, and LC3 protein levels in xenograft tumors (**e**) and in situ tumors (**f**). The tumors were isolated and then equivalent weight of samples were mixed together for further Western blot analysis. The blots shown here were on behalf of the average protein expression of six subcutaneously transplanted tumors in nude mice (**e**) or the average of nine estrogen-induced rat pituitary tumors (**f**).

ACT001 (Fig. 4b). Then Western blotting experiments were used to test the levels of phosphorylated JNK and phosphorylated P38 in rat and primary human primary pituitary tumor cell. The levels of phosphorylated JNK and P38 protein markedly increased

compared with the control group in rat pituitary tumor cells (Fig. 4c and Supplementary Fig. S3i) and the majority of ACT001-sensitive human pituitary adenoma cells (Supplementary Fig. S2b, c) after ACT001 treatment. Consistently, IHC staining showed that
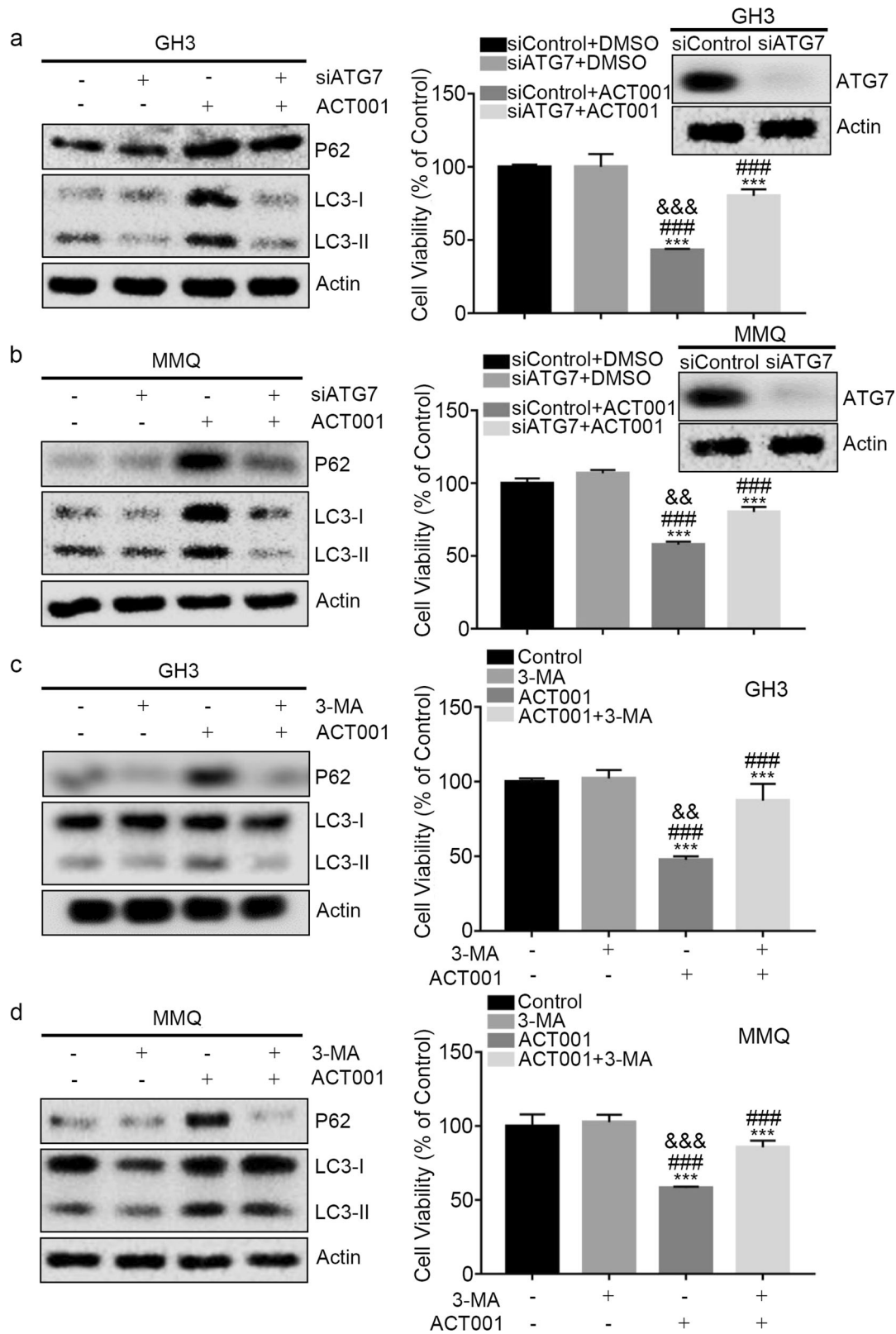
Fig. 3 **Inhibiting autophagy partially rescued ACT001-induced cell death. a, b** GH3 (**a**) and MMQ (**b**) cells were transfected with siControl or ATG7 siRNA for 48 h before treatment with ACT001 or DMSO and then subjected to immunoblot analysis for LC3, P62, and actin protein expression. **c, d** GH3 (**c**) and MMQ (**d**) cells were treated with DMSO (control) or 3-MA (3-methyladenine) for 6 h before treatment with ACT001 and then subjected to immunoblot analysis for LC3, P62, and actin protein expression. ***$P < 0.001$ vs. the siControl + DMSO or control group. ###$P < 0.001$ vs. the siATG7+DMSO or 3-MA group. &&&$P < 0.001$, &&$P < 0.01$ vs. the siATG7+ACT001 or ACT001+3-MA group.
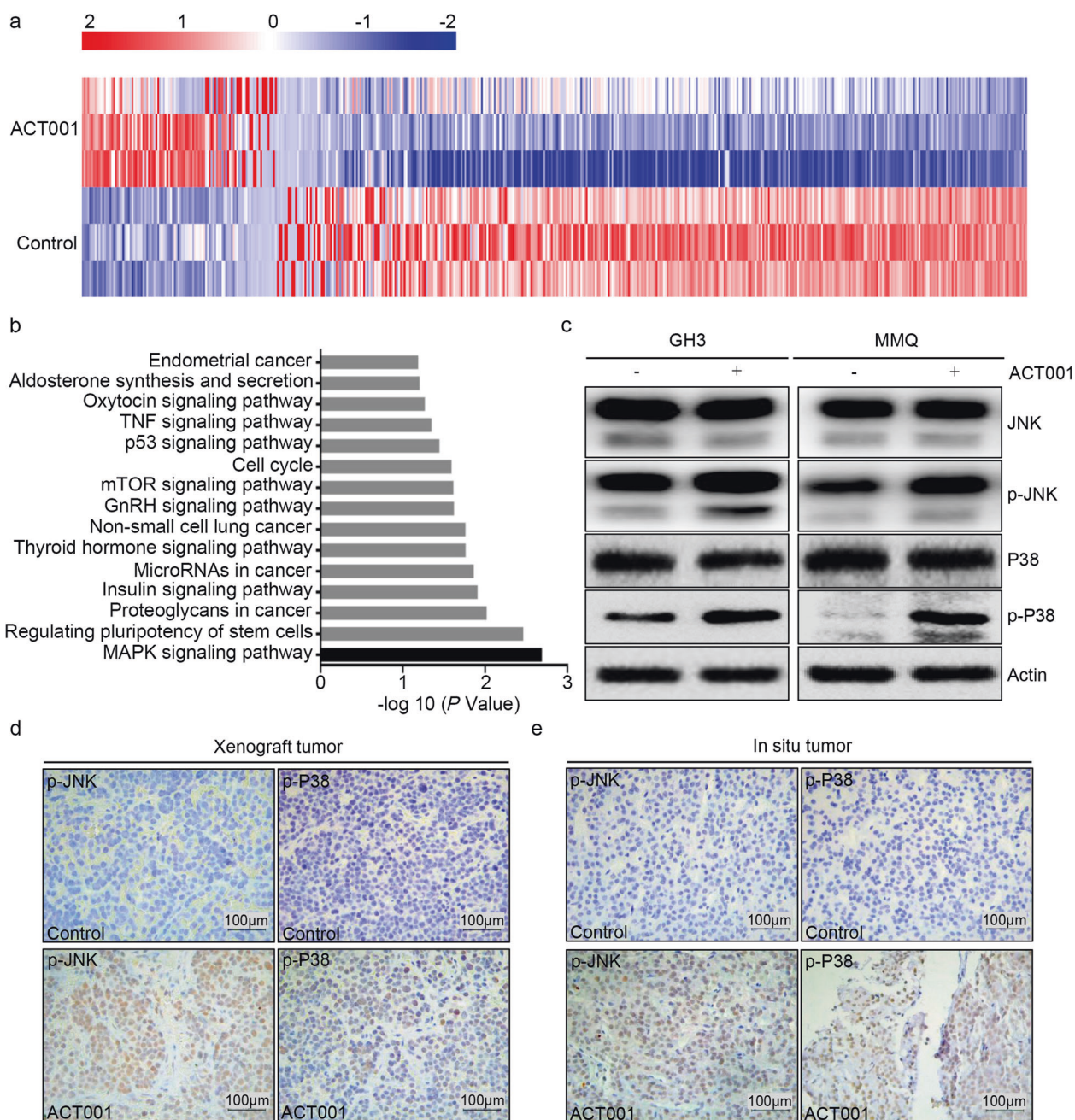
Fig. 4 **ACT001 activated the phosphorylation of JNK and P38 in pituitary tumor cells. a**, **b** RNA-seq was used to investigate the global expression profile of GH3 cells treated with ACT001 or DMSO (control) for 24 h. Heatmap (**a**) and GO analysis (**b**) showed that MAPK signaling pathway was mainly involved in the activity of ACT001. **c** Representative Western blots demonstrated that, after GH3 and MMQ cells were treated with ACT001 for 24 h, the levels of p-JNK and p-P38 markedly increased. **d**, **e** Representative images of IHC staining showed that ACT001 increased the levels of phosphorylated JNK and P38 in xenograft tumors (**d**) and in situ tumors (**e**).

the levels of phosphorylated JNK and P38 also increased in ACT001-treated group of xenograft tumors and in situ rat prolactinomas samples (Fig. 4d, e). The results above showed that ACT001 could activate the phosphorylation of JNK and P38 in pituitary tumor cell lines in vitro and in vivo.

Inhibiting the phosphorylation of JNK and P38 reversed the effect of ACT001-induced cell death
To investigate the role of JNK and P38 in ACT001-induced cell death, we used phosphorylation inhibitors of JNK and P38 in GH3 and MMQ cells. Treatment with SP600125, a phosphorylating inhibitor of JNK, inhibited ACT001-induced phosphorylation of JNK and conversion of LC3-I to LC3-II in GH3 and MMQ cells (Fig. 5a and Supplementary Fig. S3j). In cell viability assay, ACT001 treatment hindered the proliferation of tumor cells, and SP600125 partially reversed this inhibitory effect. Compared with ACT001 treatment group, the SP600125+ACT001 treatment group exhibited increased viability in GH3 cells (65.14%, $P < 0.001$, Fig. 5b, left panel) and MMQ cells (55.28%, $P < 0.001$, Fig. 5b, right panel). Similar results were also obtained after treatment with SB203580, which was P38 phosphorylation inhibitor (Fig. 5c, d and Supplementary Fig. S3k). The findings suggested that ACT001 could inhibit tumor growth by activating JNK- and P38-mediated ACD in pituitary tumors.
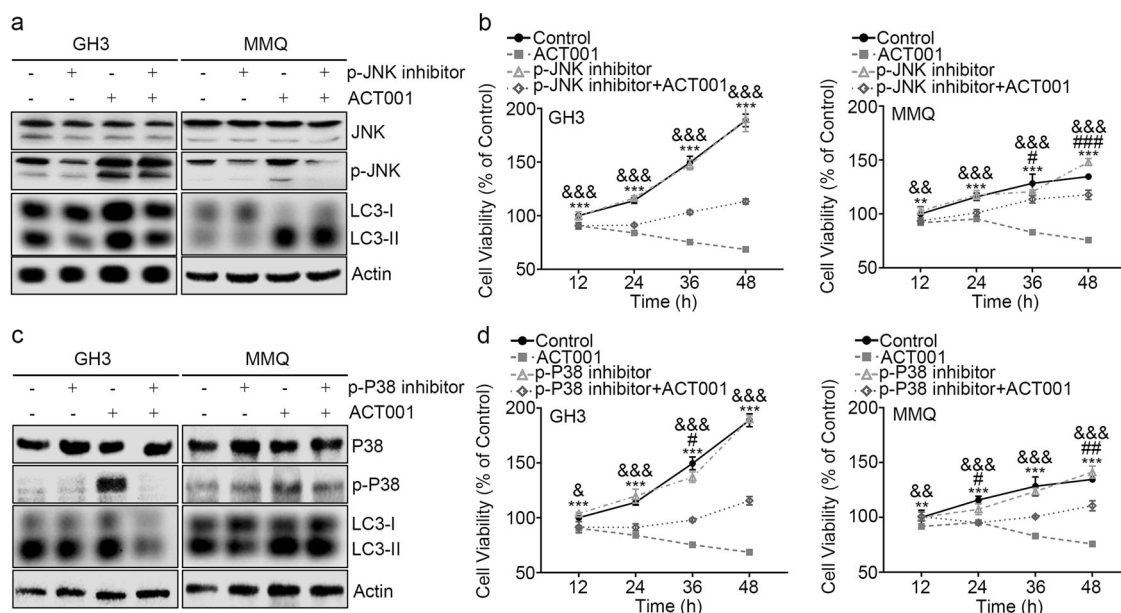
Fig. 5 Inhibiting the activation of JNK and P38 reversed the effect of ACT001. a, b MMQ and GH3 cells were treated with ACT001 in presence or absence of p-JNK inhibitor SP600125 for 24 h. **c, d** MMQ and GH3 cells were treated with ACT001 in presence or absence of p-P38 inhibitor SB203580 for 24 h. The levels of proteins were measured by Western blot, and cell survival was determined by CCK-8 assay. ***$P <$ 0.001, **$P < 0.01$ vs. the ACT001 group. ###$P < 0.001$, ##$P < 0.01$, #$P < 0.05$ vs. phosphorylating inhibitor group. &&&$P < 0.001$, &&$P < 0.01$, &$P < 0.05$ vs. phosphorylating inhibitor + ACT001 group.

ACT001 promoted the phosphorylation of JNK and P38 by binding to MEK4

To further clarify the mechanism of interaction between ACT001 and the phosphorylation of JNK and P38, an active probe and an inactive probe of ACT001 were designed and synthesized [14, 23]. Proteins bound to ACT001-biotin probe in GH3 cells were detected by LC–MS analysis. Two polypeptide segments ([R].DIKPSNILLDR.[S] and [K].WNSVFDQLTQVVK.[G]) with mass-to-charge ratios (m/z) of 642.3702 and 782.4161 were identified. These polypeptide segments were consistent with dual specificity mitogen-activated protein kinase kinase 4 (MEK4, LOCUS number: NP_001025194) from the Entrez Protein database (https://www.ncbi.nlm.nih.gov/protein, Fig. 6a, listed in Supplementary Table S4). To further verify whether MEK4 protein was precipitated by ACT001-biotin probe, the proteins pulled down by ACT001-biotin probe and ACT001-S-biotin probe in GH3 and MMQ cells were visualized by silver staining and Western blot assays. The silver staining results showed bands at ~43–45 kDa, which was similar to the molecular weight of MEK4 (Fig. 6b). Western blotting assays also confirmed that MEK4 was one of the proteins pulled down by the ACT001-biotin probe (Fig. 6c). Furthermore, after being treated with ACT001 for 24 h, GH3 and MMQ cells showed increased levels of phosphorylated MEK4 at serine 80 (Fig. 6d and Supplementary Fig. S3l).

Based on these findings, it was possible that ACT001 increased the phosphorylation level of MEK4, an upstream protein kinase of JNK and P38, at serine 80, further promoting the phosphorylation of JNK and P38 (Fig. 6e).

DISCUSSION

Despite ACT001 has been shown to possess multiple biological activities with low toxicity in the treatment of central nervous system tumors [7, 15, 26], the mechanism by which ACT001 inhibits pituitary tumor growth is still unclear. In this study, we demonstrated that ACT001 exerted a significant inhibitory effect on the growth of rat pituitary tumor cells in vitro and in vivo, as well as on primary human pituitary tumor cells. Our investigation of the mechanism underlying these effects showed that

ACT001 induced ACD through activating MEK4-mediated phosphorylation of P38 and JNK.

The guaianolide sesquiterpene lactone is the main bioactive component in ACT001, which was initially used for the treatment of fever, migraine, and arthritis [28]. In the past few years, the anti-tumor effects of ACT001 have been gradually recognized, providing a new option for treating a variety of cancer cells in clinical practice. In the treatment of glioblastoma and breast cancer, ACT001 suppressed tumor cell proliferation by inhibiting the activation of NF-κB and increasing the level of reactive oxygen species [11, 15, 24, 26]. ACT001 could restrain the metabolic reprogramming of leukemia cells by irreversibly activating pyruvate kinase M2, a key protein in the regulation of glycolysis [14]. In this study, we revealed that ACT001 could exert its inhibitory effect via inducing ACD, which have been shown to play a pivotal role in the treatment of pituitary adenomas [29, 30].

The MAPK pathway, which mainly include three subfamilies based on the conserved Thr-Xaa-Tyr motif signature—ERK1/2, P38 and JNK [31]—is a crucial regulator in cell dissemination, survival, and drug resistance of human cancers [31–33], including pituitary adenomas [34, 35]. Previous studies also demonstrated that bromocriptine (BRC) induced apoptotic cell death in pituitary tumor cells via activating P38 pathway [36, 37] and JNK activation in the pituitary gland could be associated with pituitary tumor suppression [38]. Besides, accumulating evidence has shown that the activation of P38 and JNK could promote autophagy-dependent cell death [39, 40]. Here, our data showed that ACT001 could induce ACD of pituitary tumor cells in vitro and in vivo by activating the phosphorylation of P38 and JNK. Inhibiting the activation of P38 and JNK could reverse the inhibitory effect of ACT001. However, identifying the precise mechanisms by which ACT001 induces the activation of P38 and JNK is still a challenging problem that needs to be further elucidated.

Some studies have shown that MEK4 could directly phosphorylate and activate JNK in response to environmental stress, proinflammatory cytokines and developmental cues [41]. MEK4 could also activate P38 phosphorylation, enabling the cross-talk
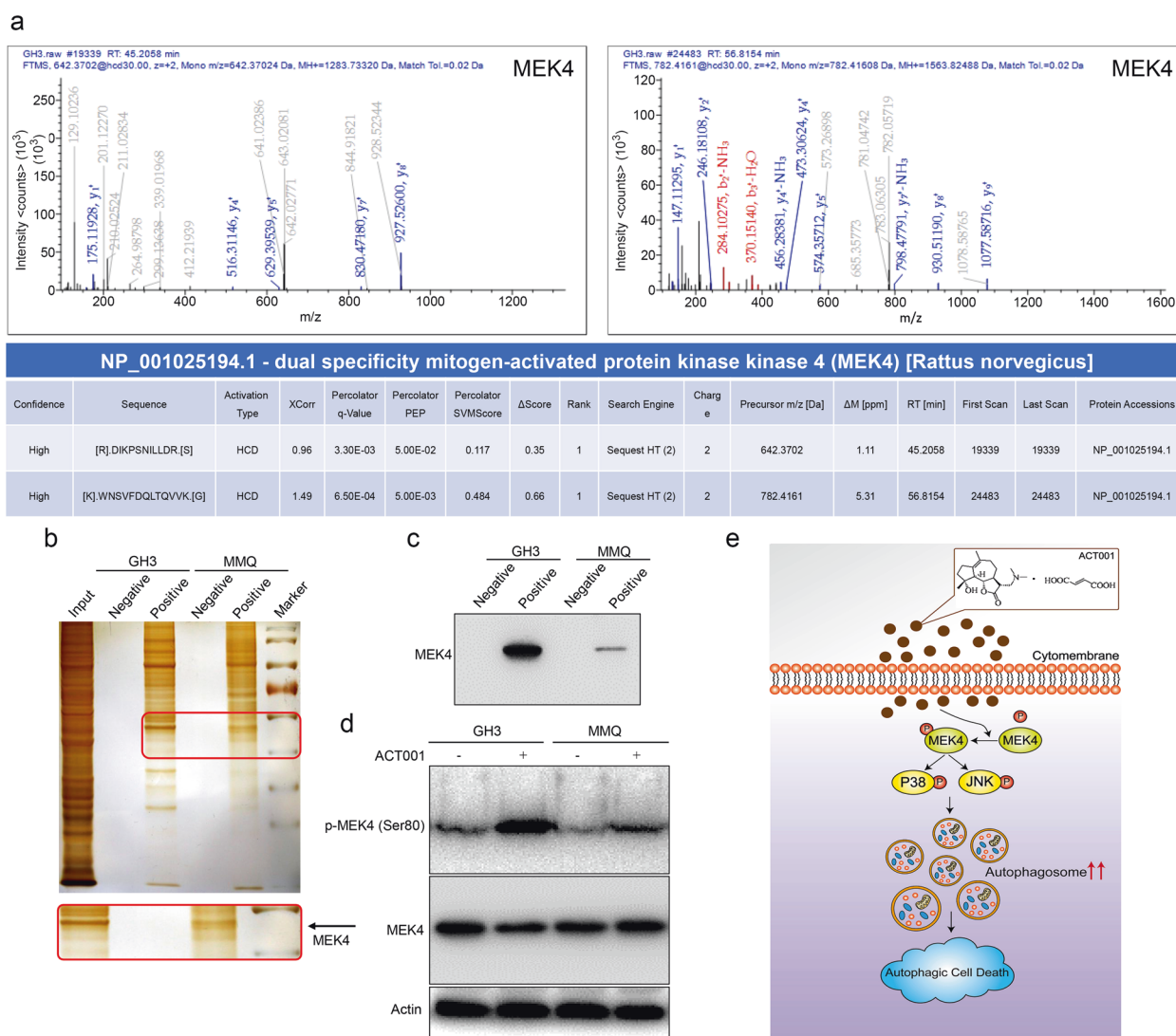
Fig. 6 ACT001 activated the phosphorylation of JNK and P38 by binding with MEK4. a Identified amino acids and peptides specific to MEK4. Proteins bound to ACT001-biotin in GH3 cells were subjected to LC–MS analysis. The LC–MS analysis data of the polypeptide segments. **b** Proteins in GH3 and MMQ cells were detected via silver staining. Input refered to the whole protein lysates from GH3 and MMQ cells; negative refered to ACT001-S-biotin probe solution; and positive refered to proteins pulled down by ACT001-biotin probe. **c** Proteins precipitated by ACT001-biotin probe or ACT001-S-biotin probe in MMQ and GH3 cells, respectively, were detected by Western blotting using an anti-MEK4 primary antibody. **d** After MMQ and GH3 cells were treated with ACT001 for 24 h, proteins were extracted and detected by Western blotting using an anti-p-MEK4 primary antibody. **e** Schematic illustration depicting that ACT001 could suppress pituitary tumor cell growth by inducing ACD via activating the phosphorylation of JNK and P38.

between the JNK signaling pathway and the P38 signaling pathway [42]. However, the mechanism by which ACT001 activates P38 and JNK remains unclear. In this study, we identified MEK4 as a new target of ACT001. ACT001 could bind to MEK4 and increase the phosphorylation level of MEK4 at serine 80 (shown in Fig. 6). Phosphorylated MEK4, which acted as a protein kinase, could further catalyze the activation of JNK and P38 signaling pathway (Fig. 6e).

DRD2 agonists, such as BRC and cabergoline (CAB), have been treated as the first-choice treatment for shrinking the volume and controlling hyperprolactinemia of prolactinomas [2]. DAs inhibit pituitary tumor cells mainly by selectively activating DRD2 [43–45]. Thus, the deficiency in DRD2 expression limits the curative effect of DAs [44, 46]. Previous studies have revealed that MMQ cells, which had relatively high DRD2 expression, were sensitive to DAs treatment. Conversely, GH3 cells, which had low/negative expression of DRD2, were considered DA-resistant cells [22, 29, 47]. In the present study, ACT001 was shown to possess a similar optimal inhibitory effect on the growth of MMQ cells and GH3 cells by inducing ACD via activating the phosphorylation of JNK and P38. ACT001 could also inhibit the growth of human primary pituitary adenoma cells, including one case of DA-resistant prolactinoma. These results suggested that, unlike the mechanism by which DAs induced cell death via activation of DRD2, ACT001 might offer a new supplementary approach for treating DA-resistant prolacti-nomas. The characteristics of ACT001 properties in central nervous system tumors have been demonstrated by previous research studies, including its minimal adverse effects and high intracranial concentration of accumulated drugs [7, 8, 15, 26]. Combined with these previous findings, our study revealed that ACT001 might have been applicable for the treatment of pituitary adenomas and be an effective complementary method for DAs treatment. Follow-up clinical trials are necessary to further evaluate its treatment value in pituitary adenomas.

In summary, this study established the anticancer effects of ACT001 on pituitary adenomas by inducing ACD through

activating the phosphorylation of JNK and P38 in vitro and in vivo. These findings provide us with novel insights into the mechanism that ACT001 plays a part in, as well as with a potential therapeutic drug for the medical management of pituitary adenomas.

AUTHOR CONTRIBUTIONS
LC: Conceptualization, methodology, investigation, and writing-original draft. ZRW: Methodology, writing-review and editing, supervision, funding acquisition. LC: Conceptualization, methodology, and investigation. JDX: Conceptualization, methodology, and investigation. JLL: Methodology, supervision, and investigation. CDW: Supervision, investigation. JHJ: Supervision, investigation. ZBW: Conceptualization, writing-review and editing, supervision. ZPS: Conceptualization, writing-review and editing, supervision, funding acquisition.

ADDITIONAL INFORMATION
Supplementary information The online version contains supplementary material available at https://doi.org/10.1038/s41401-021-00856-5.

Competing interests: The authors declare no competing interests.

REFERENCES
1. Melmed S, Casanueva FF, Hoffman AR, Kleinberg DL, Montori VM, Schlechte JA, et al. Diagnosis and treatment of hyperprolactinemia: an Endocrine Society clinical practice guideline. J Clin Endocrinol Metab. 2011;96:273–88.
2. Melmed S. Pituitary-tumor endocrinopathies. N Engl J Med. 2020;382:937–50.
3. Casanueva FF, Molitch ME, Schlechte JA, Abs R, Bonert V, Bronstein MD, et al. Guidelines of the Pituitary Society for the diagnosis and management of prolactinomas. Clin Endocrinol. 2006;65:265–73.
4. Lin S, Zhang A, Zhang X, Wu ZB. Treatment of pituitary and other tumours with cabergoline: new mechanisms and potential broader applications. Neuroendocrinology. 2020;110:477–88.
5. Zhang Q, Lu Y, Ding Y, Zhai J, Ji Q, Ma W, et al. Guaianolide sesquiterpene lactones, a source to discover agents that selectively inhibit acute myelogenous leukemia stem and progenitor cells. J Med Chem. 2012;55:8757–69.
6. An Y, Guo W, Li L, Xu C, Yang D, Wang S, et al. Micheliolide derivative DMAMCL inhibits glioma cell growth in vitro and in vivo. PLoS One. 2015;10:e0116202.
7. Lickliter JD, Jennens R, Lemech CR, Su SYC, Chen Y. Phase 1 dose-escalation study of ACT001 in patients with recurrent glioblastoma and other advanced solid tumors. J Clin Oncol. 2018;36:e14048.
8. Tong L, Li J, Li Q, Wang X, Medikonda R, Zhao T, et al. ACT001 reduces the expression of PD-L1 by inhibiting the phosphorylation of STAT3 in glioblastoma. Theranostics. 2020;10:5943–56.
9. Hou Y, Sun B, Liu W, Yu B, Shi Q, Luo F, et al. Targeting of glioma stem-like cells with a parthenolide derivative ACT001 through inhibition of AEBP1/PI3K/AKT signaling. Theranostics. 2021;11:555–66.
10. Ma WW, Shi QQ, Ding YH, Long J, Zhang Q, Chen Y. Synthesis of micheliolide derivatives and their activities against AML progenitor cells. Molecules. 2013;18:5980–92.
11. Lu C, Wang W, Jia Y, Liu X, Tong Z, Li B. Inhibition of AMPK/autophagy potentiates parthenolide-induced apoptosis in human breast cancer cells. J Cell Biochem. 2014;115:1458–66.
12. Czyz M, Lesiak-Mieczkowska K, Koprowska K, Szulawska-Mroczek A, Wozniak M. Cell context-dependent activities of parthenolide in primary and metastatic melanoma cells. Br J Pharmacol. 2010;160:1144–57.
13. Xi XN, Liu N, Wang QQ, Wu HT, He HB, Wang LL, et al. Pharmacokinetics, tissue distribution and excretion of ACT001 in Sprague-Dawley rats and metabolism of ACT001. J Chromatogr B Anal Technol Biomed Life Sci. 2019;1104:29–39.
14. Li J, Li S, Guo J, Li Q, Long J, Ma C, et al. Natural product micheliolide (MCL) irreversibly activates pyruvate kinase M2 and suppresses leukemia. J Med Chem. 2018;61:4155–64.
15. Li Q, Sun Y, Liu B, Li J, Hao X, Ge W, et al. ACT001 modulates the NF-kappaB/MnSOD/ROS axis by targeting IKKbeta to inhibit glioblastoma cell growth. J Mol Med. 2020;98:263–77.
16. Tashjian AH Jr, Yasumura Y, Levine L, Sato GH, Parker ML. Establishment of clonal strains of rat pituitary tumor cells that secrete growth hormone. Endocrinology. 1968;82:342–52.
17. Bancroft FC, Levine L, Tashjian AH Jr. Control of growth hormone production by a clonal strain of rat pituitary cells. Stimulation by hydrocortisone. J Cell Biol. 1969;43:432–41.
18. Tashjian AH Jr, Bancroft FC, Levine L. Production of both prolactin and growth hormone by clonal strains of rat pituitary tumor cells. Differential effects of hydrocortisone and tissue extracts. J Cell Biol. 1970;47:61–70.
19. Judd AM, Login IS, Kovacs K, Ross PC, Spangelo BL, Jarvis WD, et al. Characterization of the MMQ cell, a prolactin-secreting clonal cell line that is responsive to dopamine. Endocrinology. 1988;123:2341–50.
20. Lopes MBS. The 2017 World Health Organization classification of tumors of the pituitary gland: a summary. Acta Neuropathol. 2017;134:521–35.
21. Heaney AP, Horwitz GA, Wang Z, Singson R, Melmed S. Early involvement of estrogen-induced pituitary tumor transforming gene and fibroblast growth factor expression in prolactinoma pathogenesis. Nat Med. 1999;5:1317–21.
22. Wu ZR, Yan L, Liu YT, Cao L, Guo YH, Zhang Y, et al. Inhibition of mTORC1 by lncRNA H19 via disrupting 4E-BP1/Raptor interaction in pituitary tumours. Nat Commun. 2018;9:4624.
23. Xi X, Liu N, Wang Q, Chu Y, Yin Z, Ding Y, et al. ACT001, a novel PAI-1 inhibitor, exerts synergistic effects in combination with cisplatin by inhibiting PI3K/AKT pathway in glioma. Cell Death Dis. 2019;10:757.
24. D'Anneo A, Carlisi D, Lauricella M, Puleio R, Martinez R, Di Bella S, et al. Parthenolide generates reactive oxygen species and autophagy in MDA-MB231 cells. A soluble parthenolide analogue inhibits tumour growth and metastasis in a xenograft model of breast cancer. Cell Death Dis. 2013;4:e891.
25. Li S, Peng F, Gong W, Wu J, Wang Y, Xu Z, et al. Dimethylaminomicheliolide ameliorates peritoneal fibrosis through the activation of autophagy. J Mol Med. 2019;97:659–74.
26. Wang Y, Zhang J, Yang Y, Liu Q, Xu G, Zhang R, et al. ROS generation and autophagosome accumulation contribute to the DMAMCL-induced inhibition of glioma cell proliferation by regulating the ROS/MAPK signaling pathway and suppressing the Akt/mTOR signaling pathway. Onco Targets Ther. 2019;12:1867–80.
27. Klionsky DJ, Abdel-Aziz AK, Abdelfatah S, Abdellatif M, Abdoli A, Abel S, et al. Guidelines for the use and interpretation of assays for monitoring autophagy (4th edition)(1). Autophagy. 2021;17:1–382.
28. Viennois E, Xiao B, Ayyadurai S, Wang L, Wang PG, Zhang Q, et al. Micheliolide, a new sesquiterpene lactone that inhibits intestinal inflammation and colitis-associated cancer. Lab Invest. 2014;94:950–65.
29. Leng ZG, Lin SJ, Wu ZR, Guo YH, Cai L, Shang HB, et al. Activation of DRD5 (dopamine receptor D5) inhibits tumor growth by autophagic cell death. Autophagy. 2017;13:1404–19.
30. Wu Z, Cai L, Lu J, Wang C, Guan J, Chen X, et al. MicroRNA-93 mediates cabergoline-resistance by targeting ATG7 in prolactinoma. J Endocrinol. 2018;240:1–13.
31. Su B, Karin M. Mitogen-activated protein kinase cascades and regulation of gene expression. Curr Opin Immunol. 1996;8:402–11.
32. Khavari TA, Rinn J. Ras/Erk MAPK signaling in epidermal homeostasis and neoplasia. Cell Cycle. 2007;6:2928–31.
33. Kim EK, Choi EJ. Compromised MAPK signaling in human diseases: an update. Arch Toxicol. 2015;89:867–82.
34. Zhan X, Wang X, Long Y, Desiderio DM. Heterogeneity analysis of the proteomes in clinically nonfunctional pituitary adenomas. BMC Med Genomics. 2014;7:69.
35. Zhan X, Long Y. Exploration of molecular network variations in different subtypes of human non-functional pituitary adenomas. Front Endocrinol. 2016;7:13.
36. Kanasaki H, Fukunaga K, Takahashi K, Miyazaki K, Miyamoto E. Involvement of p38 mitogen-activated protein kinase activation in bromocriptine-induced apoptosis in rat pituitary GH3 cells. Biol Reprod. 2000;62:1486–94.
37. Peverelli E, Olgiati L, Locatelli M, Magni P, Fustini MF, Frank G, et al. The dopamine-somatostatin chimeric compound BIM-23A760 exerts antiproliferative and cytotoxic effects in human non-functioning pituitary tumors by activating ERK1/2 and p38 pathways. Cancer Lett. 2010;288:170–6.
38. Gong YY, Liu YY, Yu S, Zhu XN, Cao XP, Xiao HP. Ursolic acid suppresses growth and adrenocorticotrophic hormone secretion in AtT20 cells as a potential agent targeting adrenocorticotrophic hormone-producing pituitary adenoma. Mol Med Rep. 2014;9:2533–9.

2396

39. Cui Q, Tashiro S, Onodera S, Minami M, Ikejima T. Oridonin induced autophagy in human cervical carcinoma HeLa cells through Ras, JNK, and P38 regulation. J Pharmacol Sci. 2007;105:317–25.

40. Zhao M, Yang M, Yang L, Yu Y, Xie M, Zhu S, et al. HMGB1 regulates autophagy through increasing transcriptional activities of JNK and ERK in human myeloid leukemia cells. BMB Rep. 2011;44:601–6.

41. Whitmarsh AJ, Davis RJ. Role of mitogen-activated protein kinase kinase 4 in cancer. Oncogene. 2007;26:3172–84.

42. Jiang Y, Gram H, Zhao M, New L, Gu J, Feng L, et al. Characterization of the structure and function of the fourth member of p38 group mitogen-activated protein kinases, p38delta. J Biol Chem. 1997;272:30122–8.

43. Passos VQ, Fortes MA, Giannella-Neto D, Bronstein MD. Genes differentially expressed in prolactinomas responsive and resistant to dopamine agonists. Neuroendocrinology. 2009;89:163–70.

44. Wu ZB, Zheng WM, Su ZP, Chen Y, Wu JS, Wang CD, et al. Expression of D2RmRNA isoforms and ERmRNA isoforms in prolactinomas: correlation with the response to bromocriptine and with tumor biological behavior. J Neurooncol. 2010;99:25–32.

45. Roof AK, Jirawatnotai S, Trudeau T, Kuzyk C, Wierman ME, Kiyokawa H, et al. The balance of PI3K and ERK signaling is dysregulated in prolactinoma and modulated by dopamine. Endocrinology. 2018;159:2421–34.

46. Su Z, Jiang X, Wang C, Liu J, Chen Y, Li Q, et al. Differential effects of nerve growth factor on expression of dopamine 2 receptor subtypes in GH3 rat pituitary tumor cells. Endocrine. 2012;42:670–5.

47. Souteiro P, Karavitaki N. Dopamine agonist resistant prolactinomas: any alternative medical treatment? Pituitary. 2020;23:27–37.